Effect of stearic acid treatment on the properties of aligned short hemp fibre mats and their potential use as reinforcement in polypropylene matrix composites

Pickering, Kim L and Sunny, Tom*

School of Engineering, University of Waikato, Hamilton, 3240, New Zealand

*Correspondence to: Email: tomsunny54@gmail.com

Abstract

The main objective of this study was to assess the effect of stearic acid vapour treatment on hemp fibre mats produced using dynamic sheet forming (DSF), and the potential use of these treated mats as reinforcement in polypropylene matrix composites. Stearic acid was successfully applied through vapour treatment, appearing to form a layer on fibre surfaces. It was found that the presence of stearic acid increased hydrophobicity and thermal stability of fibre mats. It was also found to increase thermal stability of polypropylene matrix composites as well as their strength.

Keywords: Hemp Fibre, Dynamic Sheet Forming, Stearic acid, Polypropylene Composites

1. Introduction

Literature supports that natural plant fibres composites (NPFCs) offer a viable alternative for synthetic fibre composites due to their low environmental impact, low cost and low density. However, lack of resistance to moisture absorption limits the potential use of NPFCs for many applications. Moisture accumulation in the cell walls of natural fibres leads to fibre swelling with associated loss of dimensional stability, as well as reduction of interfacial bonding with polymer matrices (Azwa et al. 2013; Efendy and Pickering 2014). This in turn adversely affects stress transfer efficiency (matrix to fibre) for a composite during loading, leading to reduced mechanical performance (Pickering 2008).

Extensive research has been carried out to attain improved interfacial bonding in NPFCs. Chemical treatments such as alkaline, silane, acetylation and maleated anhydride grafted coupling agents are commonly seen in the literature and have the best outcomes obtained to date (Kabir et al. 2012;

Dhakal, Zhang, and Richardson 2007). Another attractive treatment reported for modifying natural fibre surfaces is stearic acid (SA) treatment. Research has shown that treatment with SA can be carried out via solution or vapour phase methods (Zafeiropoulos et al. 2002). The most popular is by solution, which involves dissolving SA in an appropriate solvent (most commonly in an ethyl alcohol solution) (Kabir et al. 2012; Li, Tabil, and Panigrahi 2007). However, the vapour phase treatment can be considered more environmentally friendly as there is no solvent involved. It has previously been reported that flax fibres that underwent vapour phase SA treatment improved stress transfer between the fibre and the matrix (polypropylene) compared to those composites with untreated fibres (Zafeiropoulos et al. 2003). Although there is extensive research (Pickering, Efendy, and Le 2015) reporting for improvement of interfacial bonding through the use of selected fibre treatments and coupling agents, as far as the authors are aware, this is the first research to assess stearic acid vapour treatment of aligned short fibre mats for reinforcement of composites.

2. Experimental

2.1 Materials

Stearic acid, in powder form, with molecular weight of 284.48 g/mol was purchased from Merck Schuchardt, Germany. The matrix was PP random copolymer SKRX3600 with a melt index of 18 g/10 min and density of 0.9 g/cm^3 provided by Clariant (New Zealand) Ltd. The coupling agent used was A-C 950P maleic anhydride polypropylene (MAPP) supplied by Honeywell International Inc., USA.

2.2 Methods

Production of fibre mats including alkali treatment of hemp fibres, including the high temperature treatment (HT/120 °C) used is detailed in published work (Sunny, Pickering, and Lim 2020).

2.2.1 The stearic acid vapour treatment

Prior to stearic acid (SA) vapour treatment, the fibre mats to be treated were dried overnight at 80 °C. The SA treatment for the mats was carried out using a vapour process. 4 g of stearic acid was spread onto an aluminium tray. The fibre mats to be treated were left on a wire mesh that was temporarily fitted to the top of the tray, as shown in Fig. 1. The set up was entirely covered using an oven bag and sealed, and then placed in a preheated oven at 105 °C for 36 h; the treatment time and temperature were selected from a previous study that reported improved stress transfer for NPFCs (Zafeiropoulos et al. 2002). After the treatment, the mats were removed from the mesh and then oven dried at 50 °C for 12 h. The weight percentage gain from the treatment was calculated based on the dry weight of the untreated fibre mats.

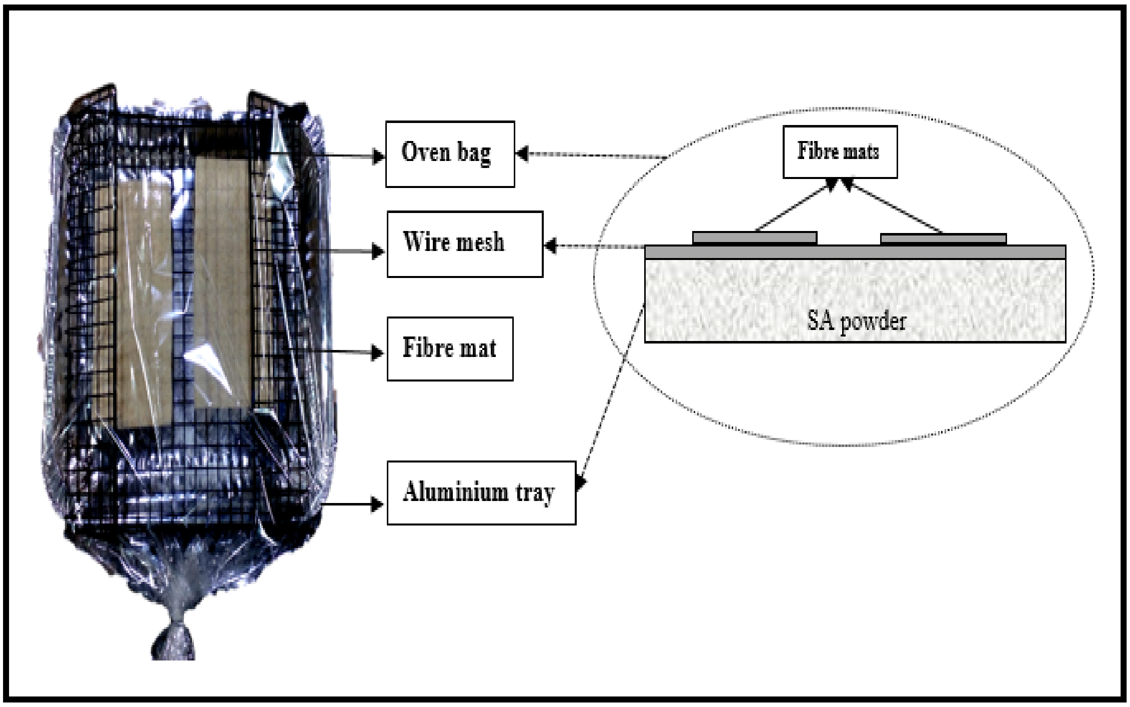

Fig. 1: Setup used for the stearic acid (SA) vapour treatment.

2.2.2 Production of PP/MAPP sheets

PP blended with MAPP was formed into sheets using a ThermoPrism TSE-16-TC twin screw extruder attached with a sheet die. The five heating zones at the extruder barrel temperatures were set at 145 °C (feed entrance), 160 °C, 155 °C, 160 °C, 170 °C (feed exit). The twin screws were operated at 45 rpm.

2.2.3 Assessment of fibre mats and composite morphology

The fibre mat surfaces and the microstructure of the tensile fracture surfaces of the samples were assessed using a Hitachi S-4100 field emission scanning electron microscope operated at 5 kV. Before observation, all samples were mounted on aluminium stubs using carbon tapes and then sputter-coated with platinum to make them conductive.

2.2.4 Fourier transform infrared spectroscopy

A PerkinElmer Spectrum One spectrometer was used to obtain the infrared spectra of the samples. The fibre mat samples were ground to fine powder using a Retsch MM400 ball mill. The ground powder for each sample was then mixed and compressed with KBr (potassium bromide) using a hydraulic press to form a disc for FTIR analysis. Neat stearic acid was also analysed.

2.2.5 Water retention value test

Water retention value (WRV) of fibre mat surfaces was characterised using a method previously reported for characterising fibre surfaces with stearic acid treatment (Kalaprasad et al. 2004). For the test, 500 mg of fibre mat was placed in a test tube with 3 ml of distilled water and shaken for 10 minutes. The mat was manually taken out from the test tube and then the wet weight of the mat (w_1) was measured. The mats were then dried in an oven at 105 °C for 24 h to obtain the dry weight of the mat (w_2). Three replicate samples were tested for each batch and average values are reported. The following equation has been used to determine the water retention value:

$$\mathrm{WRV} = \frac{(w_1 - w_2)}{w_2} \qquad (1)$$

2.2.6 Contact angle measurement

Contact angle was assessed for neat PP and PP/MAPP sheets and fibre mats. A simple custom experimental set up, as schematically shown in Fig. 2, was constructed which allowed the measurement of contact angle with reasonable precision (Lamour et al. 2010). The images for analysis were captured using a digital mobile camera. A cardboard box was employed for shielding the liquid droplet (distilled water) from air contaminants and stray light. Additionally, a commercial lamp along with a filter paper (diffuser) was positioned behind the liquid droplet for uniform lighting. Measurements were carried out on samples of dimensions 25 x 25 mm at room temperature. The measurements were repeated three times for each batch.

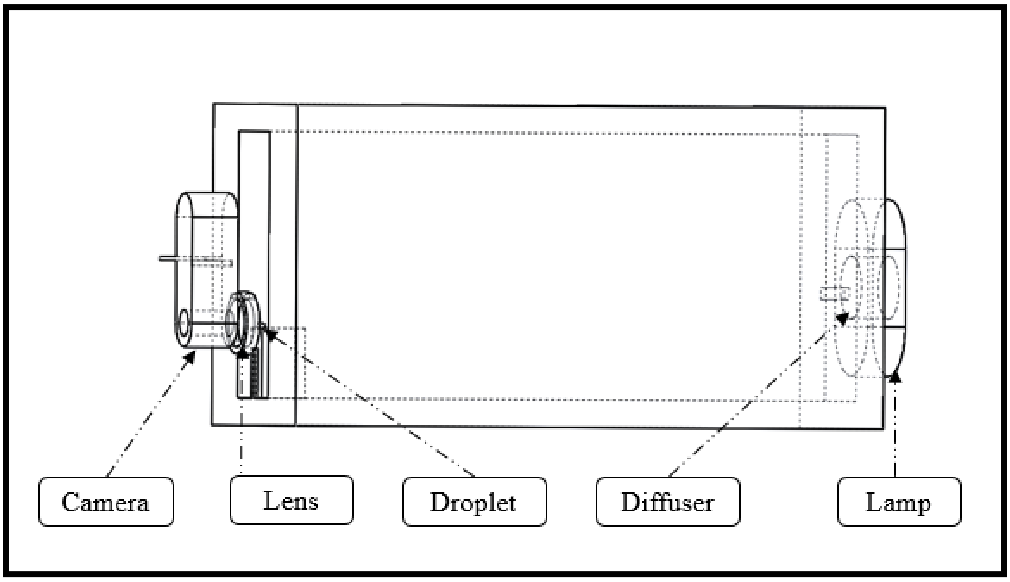

Fig. 2: Schematic diagrams of contact angle measurement set up.

2.2.7 Composites production

Composite production is detailed in published work (Sunny, Pickering, and Lim 2020). Composites with fibre contents of approximately 15 and 30 wt% were prepared. An example of a moulded composite is shown in Fig. 3. Neat PP samples were also produced for comparison purposes. Stacks of neat PP samples were heated and pressed in a hot press the same as that of PP/MAPP (the control) and composite samples (at 170 °C for 5 minutes at 1 MPa).

Fig. 3: Hemp composites with 30 wt% fibre content fabricated by compression moulding.

2.2.8 Composites tensile testing

The procedure detailed in ASTM D 638-03; Standard Test Method for Tensile Properties of Plastics was followed for tensile testing of specimens. In advance of tensile testing, all the samples were conditioned at 23 °C ± 3 °C and 50 % ± 5% relative humidity for at least 48 hours. An Instron-4204 tensile testing machine fitted with a 5 kN load cell was used for the testing. The gauge length of the specimens was 80 mm. An Instron 2630-112 extensometer with a gauge length of 50 mm was attached to the central part of the test specimen for the measurement of strain. The specimens were tested at a cross-head speed of 1 mm/min. A total of five samples were tested from each batch. Details and abbreviations of the samples used can be seen in Table 1. Five samples for each batch of composites were tested.

Table 1: Abbreviations used for PP, PP/MAPP and composite samples

Sample	Abbreviation
Neat Polypropylene	PP
PP blended with MAPP coupling agent (the control)	PP/MAPP
PP matrix composite reinforced with alkali-treated hemp	PP/H#
PP matrix composite reinforced with alkali-stearic acid-treated hemp	PP/H#/SA
PP/MAPP matrix composite reinforced with alkali-treated hemp	PP/MAPP/H#
PP/MAPP matrix composite reinforced with alkali-stearic acid-treated hemp	PP/MAPP/H#/SA

Note the following: 'H' refers to hemp fibre and the '#' following 'H' is equal to the nominal weight percentage of fibres in composites. For instance, H15 = 15 wt% hemp fibre in composites.

2.2.9 Thermogravimetric analysis

3 mg and 15 mg samples were taken from each type of fibre mat and composite, respectively and analysed using a PerkinElmer STA 8000. A scanning range of 40 to 500°C with a constant heating rate of 10°C/min and air flow at 20 ml/min were used to obtain the data.

2.2.10 Swelling testing

Swelling testing was conducted according to methodology reported in the literature (Ghazali and Efendy 2016). Samples with nominal dimensions of 30 x 5 x 3 mm were used. The initial weight, w, and wet weights after immersion in solvent for 48 h at room temperature, w_s, of three replicate samples were measured and average values for weight of solvent absorbed, A_s , reported. The swelling index of the composite was calculated using the following equation:

$$\text{Swelling Index, \%} = \frac{A_s}{w}\ x\ 100 \qquad (2)$$

where $A_s = w_s - w$

3.0 Results and Discussion

3.1 Microscopic evaluation of hemp fibre surfaces

SEM micrographs of hemp fibre surfaces are shown in Fig. 4. As can be seen in Fig. 4a, the untreated (UT) fibres are in fibre bundle forms. In contrast, high temperature alkali treated fibres (HT) appeared to have undergone separation from their bundles (Fig. 4 4b) due to the removal of localised components on their surfaces, revealing a rough texture with a large number of grooves (Fig. 4c). It appears that the stearic acid vapour treatment (HT/SA) resulted in smoother fibre surfaces (Fig. 4d compared to Fig. 4c). Furthermore, it may be seen that the fibre surfaces appeared to be covered by a thin layer. This thin layer could be attributed to the presence of stearic acid, which has been deposited on the fibre surfaces. Similar observations have been reported elsewhere (Zafeiropoulos et al. 2002).

To further investigate this deposition, the fibres treated with alkali only and further treated with stearic acid were separately exposed to electron beams under high magnification for the same exposure time (5 s). Three replicate samples were tested. The stearic acid treated fibres appeared to have undergone less damage than that of the alkali only treated fibres (Fig. 4f compared to Fig. 4e). suggesting that the stearic acid provided some protection.

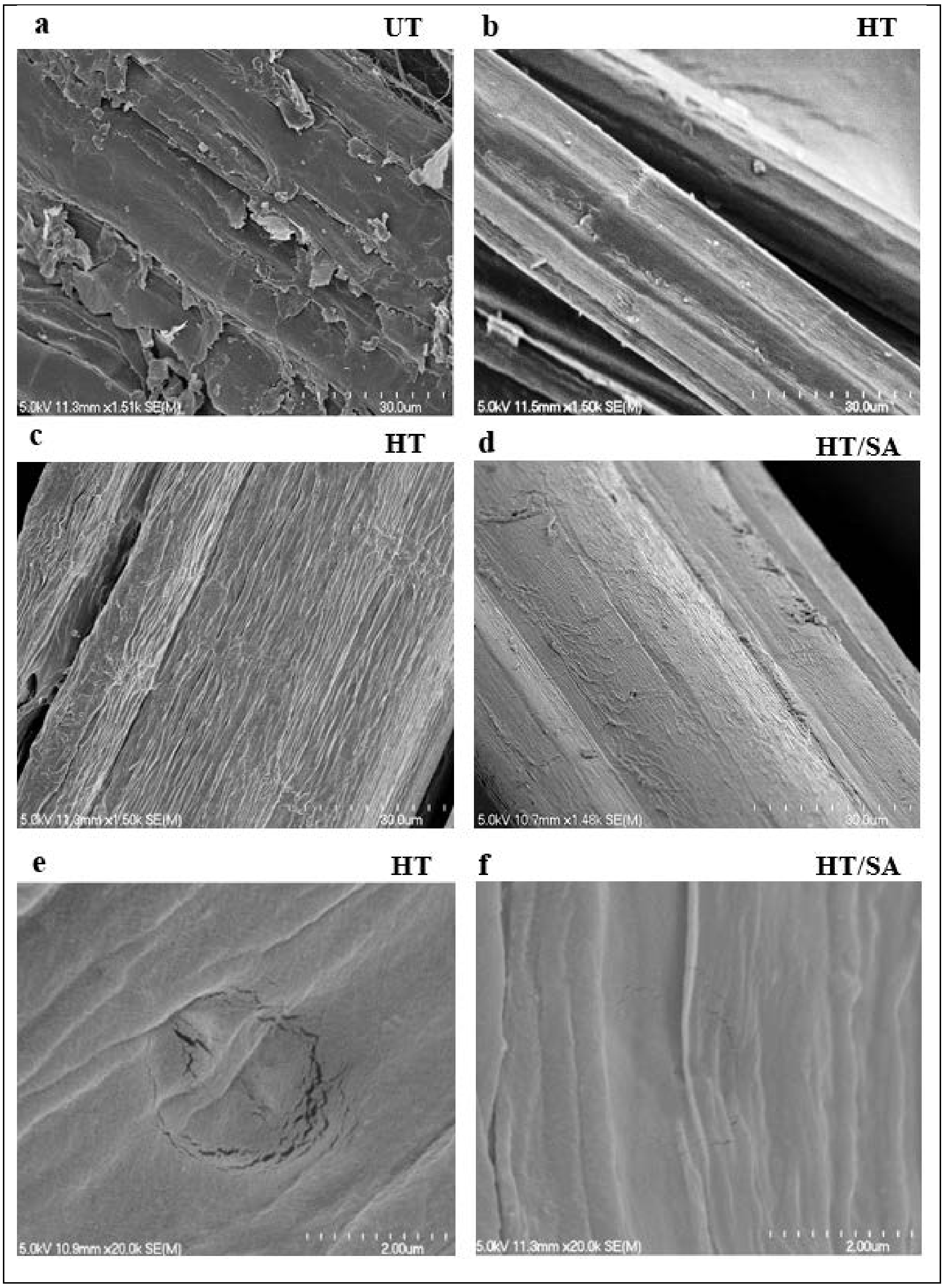

Fig. 4: **Scanning electron micrographs of fibre mats: (a) Untreated (UT), (b), (c) and (e) fibres treated with alkali only, HT and (d) and (f) fibres further treated with stearic acid, HT/SA. Note the following: HT - high temperature, SA - stearic acid, HT/SA - both HT alkali and SA treated.**

3.2 Fourier transform infrared spectroscopy

Detailed comparison of spectra of untreated (UT) and fibres treated with alkali only (HT) have been provided in published work (Sunny, Pickering, and Lim 2020). Fig. 5 shows the spectra of fibre (alkali treated) mats without stearic acid (HT) and with stearic acid (HT/SA) and neat stearic acid. In the spectra of neat stearic acid, high intensity peaks were detected at 1228-1235, 1470, 1705, 2850 and 2920 cm^{-1} which are commonly assigned in the literature to the carboxylic acids (Hernández et al.

2019). A few minor differences can be seen between the spectra of the fibre mats; two peaks related to the stretching vibrations of CH_2 groups at 2850 and 2920 cm^{-1} were more pronounced in the spectra of fibre mats with stearic acid than those without stearic acid supporting the presence of stearic acid on the fibre surfaces (Zeng et al. 2013). Assessment of whether reaction between stearic acid and the fibre had occurred was conducted, for which peaks would expected to appear at around 1733 (C=O) and 1000-1300 (C-O) cm^{-1} (Huang et al. 2018). However, such peaks were not noticeable in the spectra of fibre mats with stearic acid treatment. These observations were similar to the work reported for flax fibres treated with stearic acid vapour (Zafeiropoulos et al. 2003). The absence of ester functional groups peaks from the spectra could be due to the very low levels of stearic acid deposited on the fibre surfaces; the weight percentage gain in the fibre mats obtained after the SA treatment was around 0.54 % and so the presence of ester bonding between stearic acid and the fibre was inconclusive.

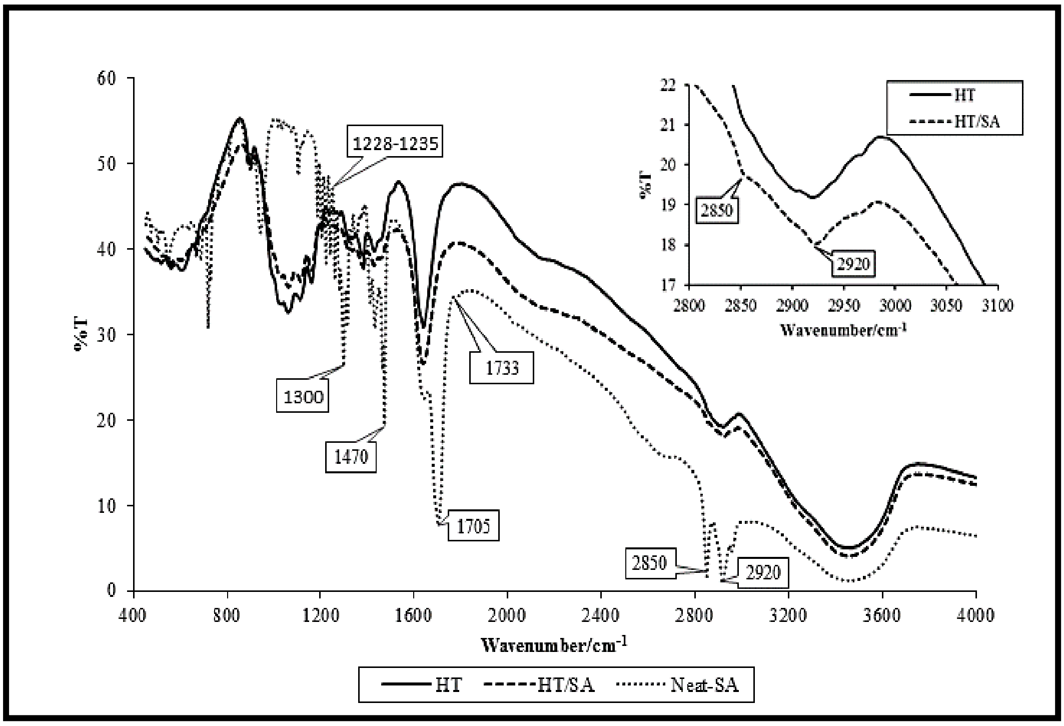

Fig. 5: FTIR-spectra of fibre mats: fibres treated with alkali only (HT), fibres treated further with stearic acid (HT/SA), and neat stearic acid. Note the following: HT - high temperature and SA - stearic acid.

3.3 Water retention values

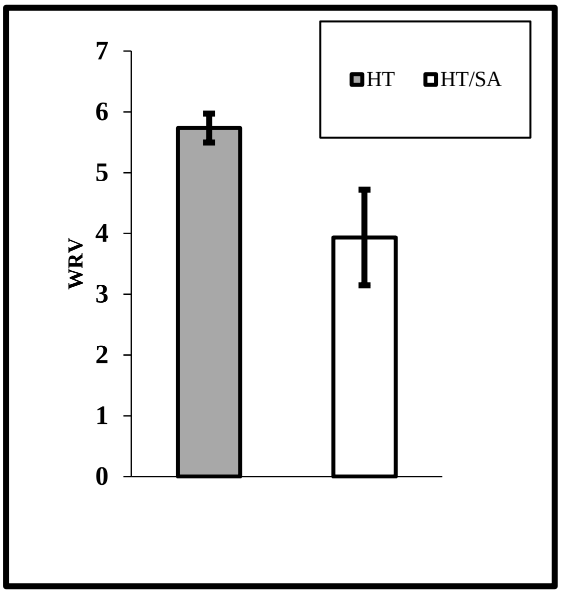

Fig. 6: Water retention values of fibre mats: fibres treated with alkali only (HT), fibres treated further with stearic acid (HT/SA).

Fig. 6 represents the average water retention values (WRVs) obtained for the fibre mats without (HT) and with SA treatment (HT/SA). As can be seen, the water retention value was significantly lower for the SA treated fibre mats compared to the fibre mats without SA treatment. This indicates that the fibre surfaces become less hydrophilic with the deposition of stearic acid. It has been previously reported that the presence of stearic acid on the fibre surfaces could reduce the fibre wetting by water (Kalaprasad et al. 2004).

3.4 Contact angle measurements

Contact angle measurements for neat PP, PP/MAPP sheets and fibre mats without (HT) and with SA treatment (HT/SA) are presented in Table 2. As expected, the neat PP films exhibited the characteristics of hydrophobic surfaces with a contact angle of 116°C. When PP was blended with MAPP, a significant decrease in the contact angle (88°) was observed. This is most likely due to the polar functional group (MA) available on the surfaces of PP/MAPP sheets as a result of blending (Beckermann 2007). It has been previously reported that the availability of polar functional groups on the film surfaces influences wettability by water (Conceição et al. 2019). Unsurprisingly, the test liquid (water, Fig. 7a) drop spontaneously spreads onto to the HT fibre mats (see Fig. 7b, left). In contrast, the water droplets were stable on the fibre mat surfaces that underwent the SA treatment (Fig.

7b, right) with the largest contact angle of 126° which is assumed to be due to the thin layer of SA deposited on the fibre mat surfaces changing the innate hydrophilic characteristics of fibre mat surfaces to become hydrophobic.

Table 2: Summary of contact angle measurements. Standard deviations are shown in parentheses. CA = contact angle

Samples	CA-Left/°	CA-Right/°	Average CA
Neat PP	115.8 (3.6)	117.0 (3.2)	116.4 (3.4)
PP/MAPP	86.8 (1.9)	89.9 (1.9)	88.4 (1.9)
HT	0	0	0
HT/SA	126.3 (1.5)	127.3 (5.1)	126.8 (3.3)

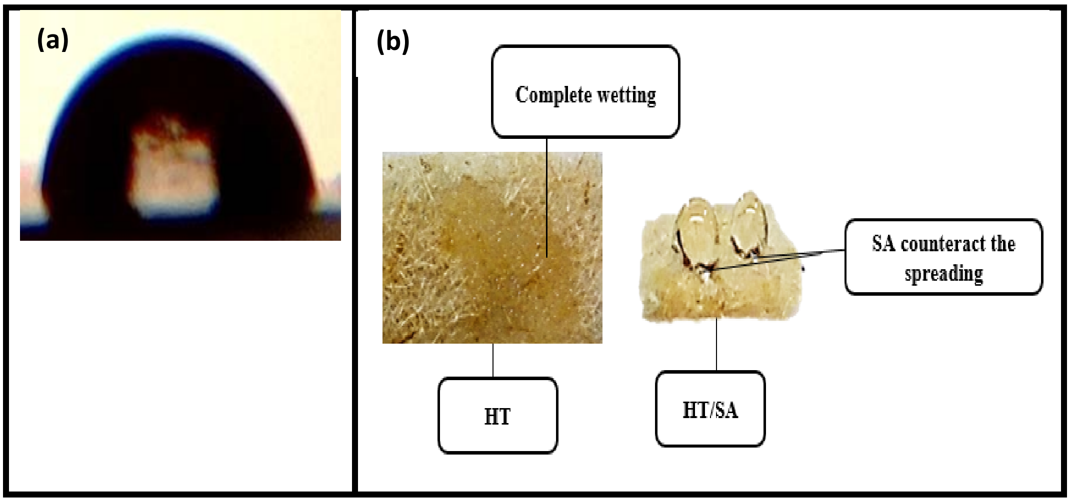

Fig. 7: (a) A sample image of water droplet used in the measurement of CAM (b) Photograph images fibre mats without and with the SA treatment.

Overall, from SEM, FTIR, weight percentage gain, WRV and contact angle measurements it may be concluded that stearic acid is present on the fibre surfaces and is more likely to be in the form of thin layers.

3.5 Composites tensile properties

The mechanical properties of the composites tested parallel and perpendicular to main fibre orientation direction are detailed in published work (Sunny, Pickering, and Lim 2020). Fig. 8a represents the tensile strengths of neat PP, PP/MAPP and the composites. Composite tensile strengths normalised by the weight percentage of fibre is shown in Fig. 8b to confirm the change in tensile strength for composites due to SA addition. It was found that the tensile strength of neat PP was not significantly affected with the addition of MAPP as confirmed by a Student's t-test, although the average tensile strength increased slightly. Table 3 details the percentages of improvement obtained for the average tensile strengths of composites from fibre inclusion, further fibre treatment (SA treatment, but not MAPP), coupling agent (MAPP) and the combination of SA and MAPP, along with those values for composites treated with alkali only (no MAPP and no SA) for comparison. The inclusion of fibres into neat PP was found to significantly increase the tensile strengths of composites.

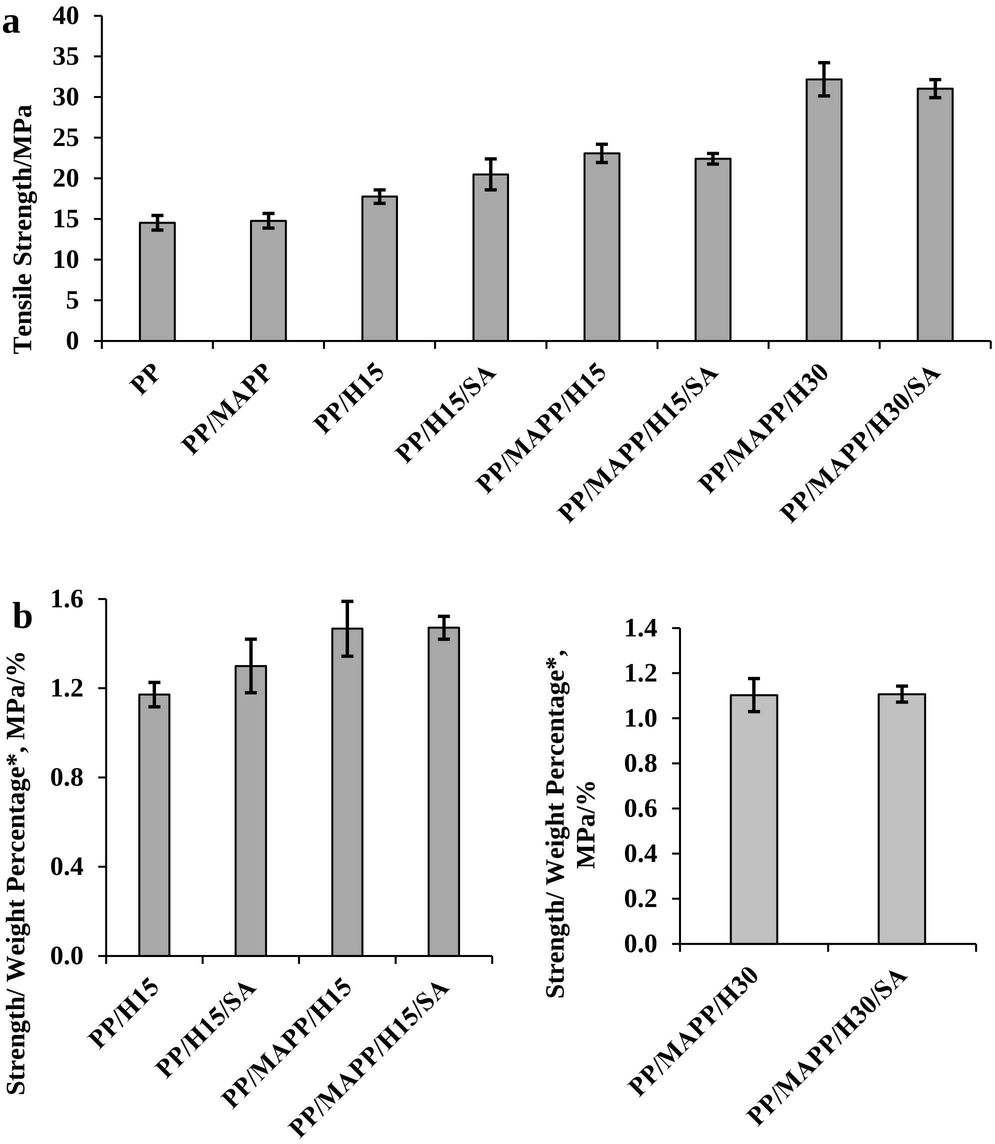

Fig. 8: (a) Tensile strength of composites as a function of various treatments (b) Tensile strength/weight percentage* of the composites. Note the following: composites were approximately 15 and 30 wt%, Weight percentage* = weight percentage of fibre mats with or without SA, SA = stearic acid and MAPP = maleic anhydride polypropylene.

Table 3: Percentage improvement in tensile strengths of composites over composites with alkali treated fibre mats only

Samples	Average tensile strength/MPa	Improvement/%
PP/H15	17.7	-
PP/H15/SA	20.4	15.3
PP/MAPP/H15	23.1	30.5
PP/MAPP/H15/SA	22.9	29.4

Average tensile strengths for composites with fibres treated using stearic acid and composites coupled with MAPP, and the combination of SA and MAPP were higher compared to those treated with alkali only. The composites with fibres treated with SA (but not MAPP) have shown significant improvement in tensile strengths; increased by about 15 % compared to those composites with fibres treated using alkali only. The composites coupled with MAPP had the highest improvement in tensile strengths; increased by approximately 31 % compared to those composites with fibres treated using alkali only. However, composites with the combination of SA and MAPP did not show further improvement compared to composites coupled with MAPP only (see Fig. 8b).

The improvement in tensile strengths for composite with fibres treated with SA (without MAPP) from various studies seen in the literature is believed to be due to improved compatibility resulting in improved fibre wetting by the matrix (Zafeiropoulos et al. 2003). As aforementioned, the fibre surfaces were less hydrophilic after the SA treatment supporting better interfacial compatibility between the fibre and the matrix than for the fibres with alkali treatment only (Zafeiropoulos, Baillie, and Matthews 2000; Dányádi, Móczó, and Pukánszky 2010). The possible interactions between the fibre surfaces, stearic acid and the matrix are shown in Fig. 9a. The SA could react with available OH groups on the fibre surfaces to form ester bonds (Raj et al. 1989). There are chances of partial entanglements of aliphatic chains of SA with the polymer chains of the matrix (PP) [8, 22]. Furthermore, the stearic acid molecules present on the fibre surfaces may reduce volatiles such as moisture from being adsorbed onto the fibres. The volatiles can desorb easily at the processing temperature of NPFCs, resulting in voids leading to the poor fibre-matrix interfaces [23].

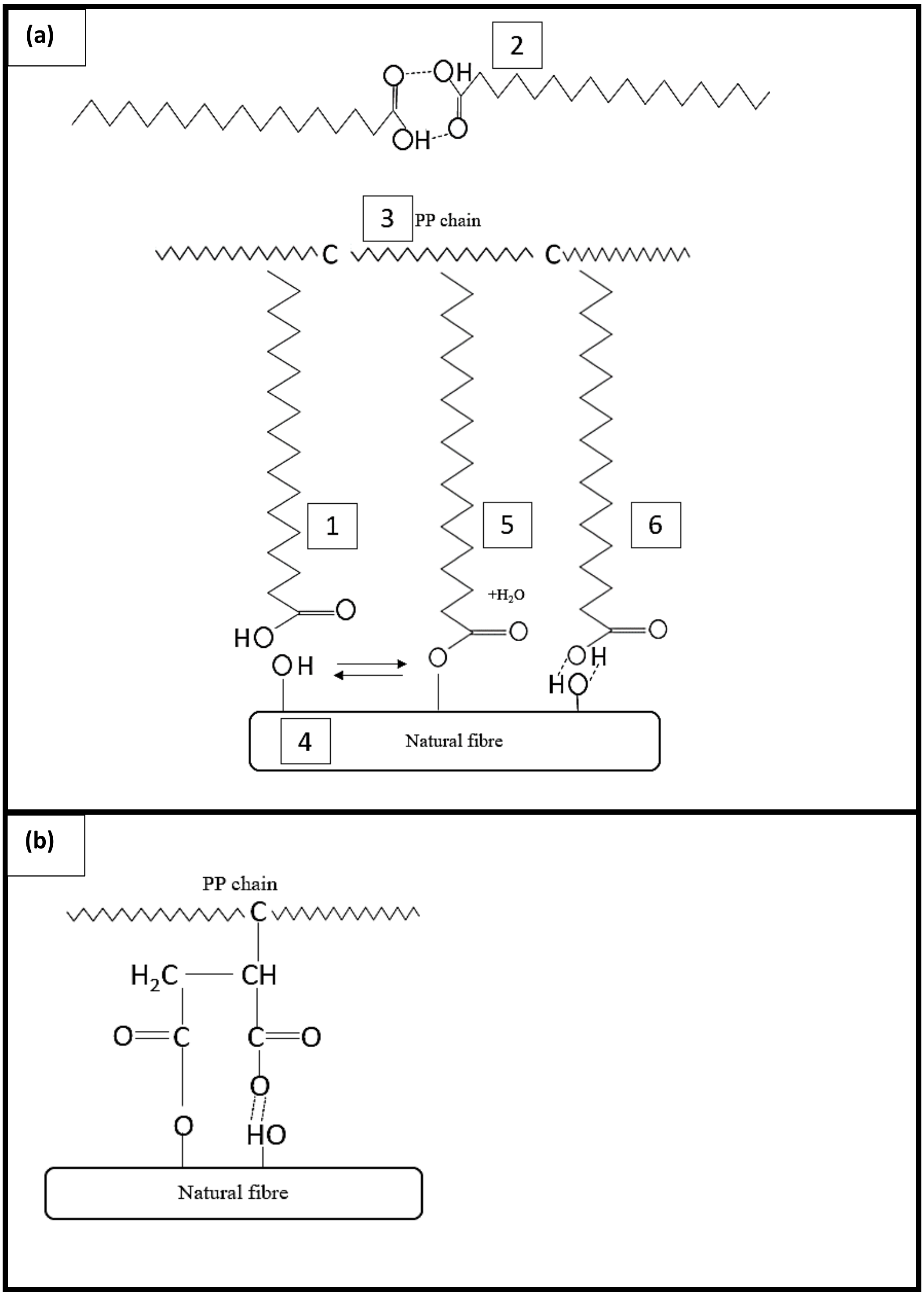

Fig. 9: Possible interactions of (a) stearic acid, natural fibre and PP (1 - neat SA, 2 - SA dimer, 3 - neat PP, 4 - natural fibre surfaces, 5 - ester bond formed with fibre surfaces, 6 - potential of hydrogen bonding), 1 and 3- partial entanglements of aliphatic chains of SA with the polymer chains of PP) (b) MAPP and OH groups on the natural fibre surfaces.

The highest improvement of tensile strength obtained was for composites with MAPP. As is well documented, MAPP acts as a bridge between the matrix and the fibres, improving the fibre-matrix adhesion, thus facilitating better stress transfer to provide improved tensile strength. Coupling occurs though the anhydride group (MA monomers) at one end which can react strongly through strong covalent ester-linkage plus potential hydrogen with the hydroxyl group present on the fibre surfaces (Fig. 9b), whilst the long polymer chains of MAPP can interact with the PP by means of chain entanglement.

Although the composites with the combination of SA and MAPP did not show further improvement of tensile strength over that obtained using just MAPP, the standard deviation for tensile strength was smaller. This suggests that the combination of better fibre wetting due to stearic acid and improved bonding through MAPP results in more consistent interaction between fibre and matrix.

Fig. 10a shows Young's modulus for neat PP, PP/MAPP and all composites tested. Similar to the tensile strength, Young's modulus of the composites was normalised by the fibre weight percentage as shown in Fig. 10b. As for tensile strength, the addition of MAPP did not significantly affect Young's modulus of neat PP. Only slight improvement in Young's modulus for composites with fibres treated with SA and composites coupled with MAPP and the combination of SA and MAPP is obtained. This suggests that the improvement in interfacial strength did not substantially influence Young's modulus for composites (Beckermann 2007; Ghazali and Efendy 2016).

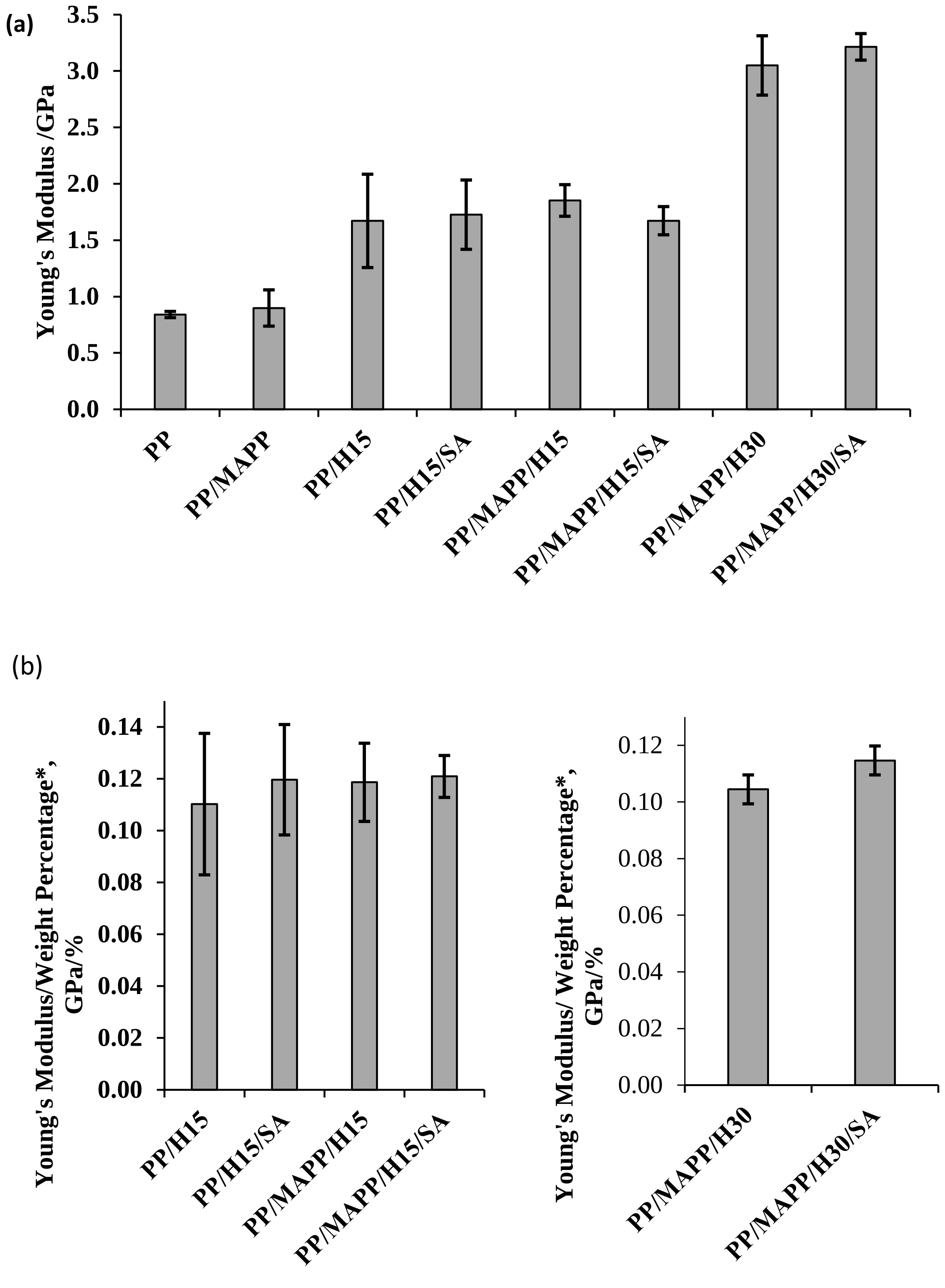

Fig. 10: (a) The Young's modulus of various composites as a function of various treatments (the composites were approximately 15 and 30wt %) (b) Young's modulus/weight percentage* of composites. Weight percentage* = weight percentage of fibre mats with or without SA.

Scanning electron micrographs of tensile fractured surfaces for composites are shown in Fig. 11. The composites with fibres treated with alkali only (Fig. 11a) had lots of fibre pull-out with large holes, suggesting very weak fibre/matrix interfacial adhesion. In contrast, that the composites with SA treated fibres without MAPP (Fig. 11b) had much less pull-out suggesting improved fibre/matrix interfacial adhesion relating to improved fibre wetting. Even less pull-out was observed with MAPP (Fig. 11c) supporting improved fibre/matrix interfacial adhesion; very few short fibres were observed at the interface as the majority of the fibres are covered up by the matrix. Little change was observed for composites with the combination of SA and MAPP (Fig. 11d) suggesting similar fibre/matrix interfacial adhesion.

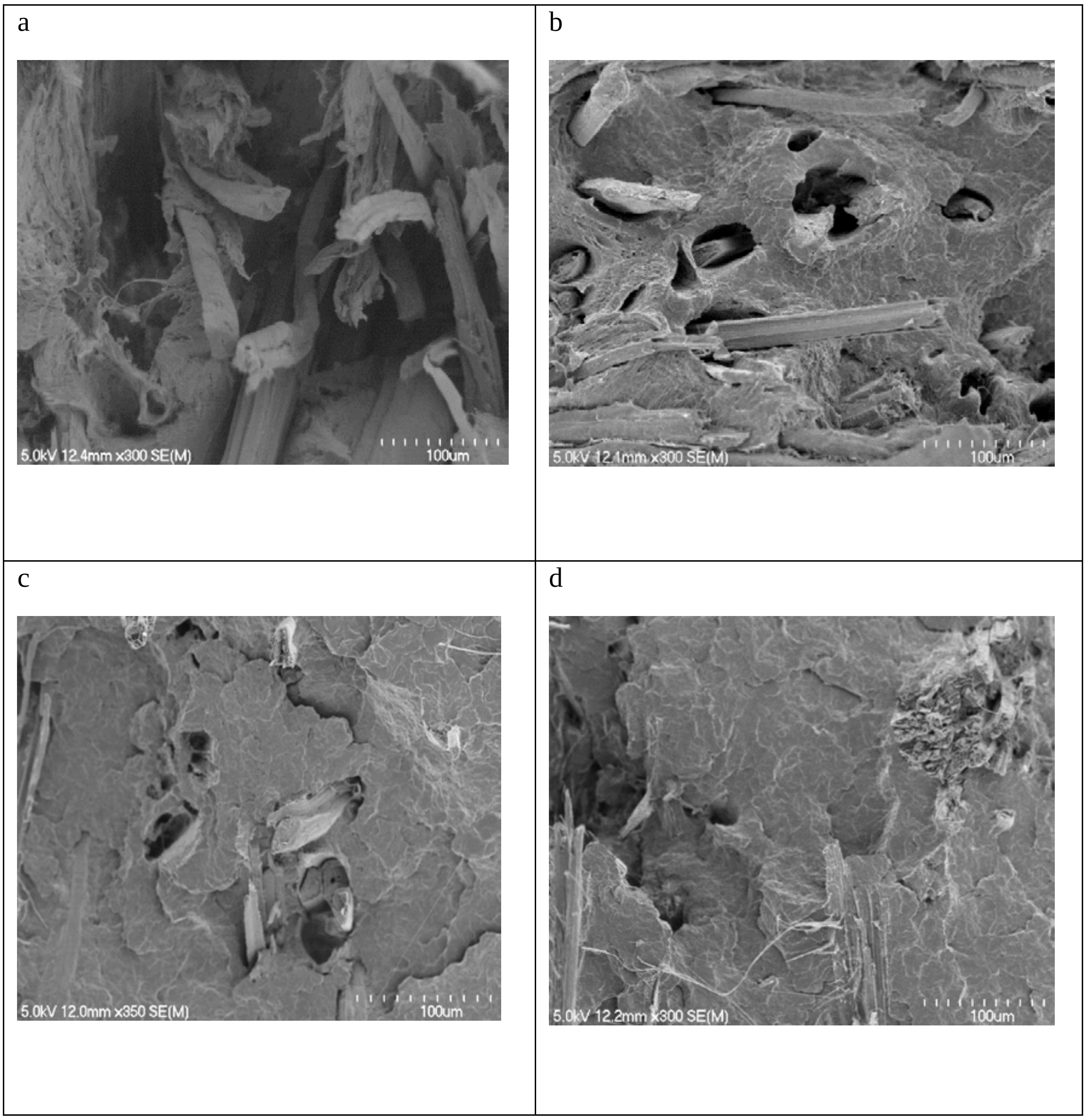

Fig. 11: SEM images of tensile fracture surfaces for composites: (a) with fibres treated with alkali only (b) with fibres further treated with SA, (c) with coupling agent MAPP and (d) with the combination of SA and MAPP.

3.6 Thermogravimetric analysis of fibre mats and composites

The TGA curves for the fibres without (HT) and with SA treatment (HT/SA) are shown in Fig. 12a; fibre weight was maintained for the fibres until around 328°C and 332°C, respectively. By 380°C, the fibres without SA treatment had lost almost 93% of their initial weight compared with 86% for fibres with SA treatment indicating improved thermal stability of fibres with SA treatment. Improvement has also been seen in the literature using SA such that SA vapour treatment had a profound effect on the thermal stability of the fibres (Zafeiropoulos, Baillie, and Matthews 2000). This could be explained by SA reducing the oxidative decomposition of charred residue (Rachini et al. 2009). However, as the thermal degradation of cellulosic materials is complex, more research would be required to elucidate the mechanisms involved.

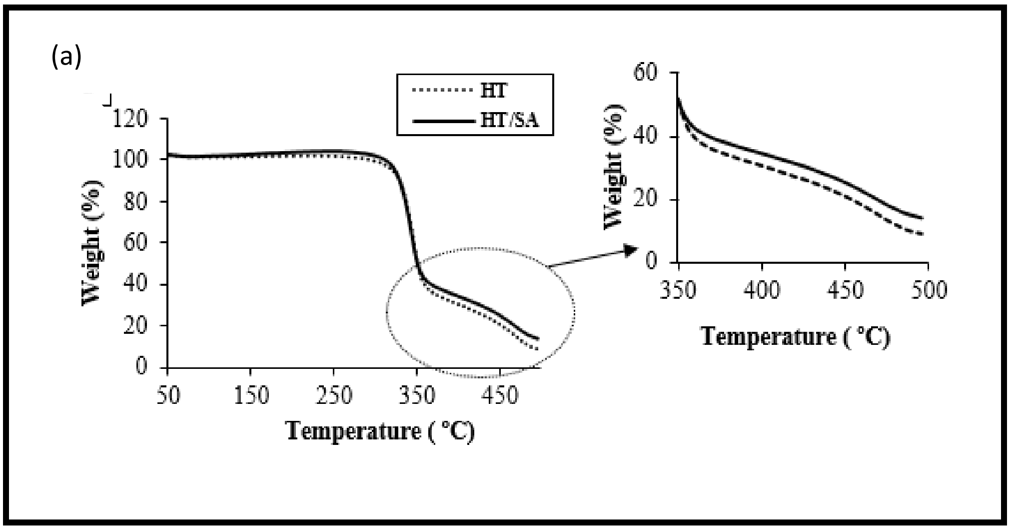

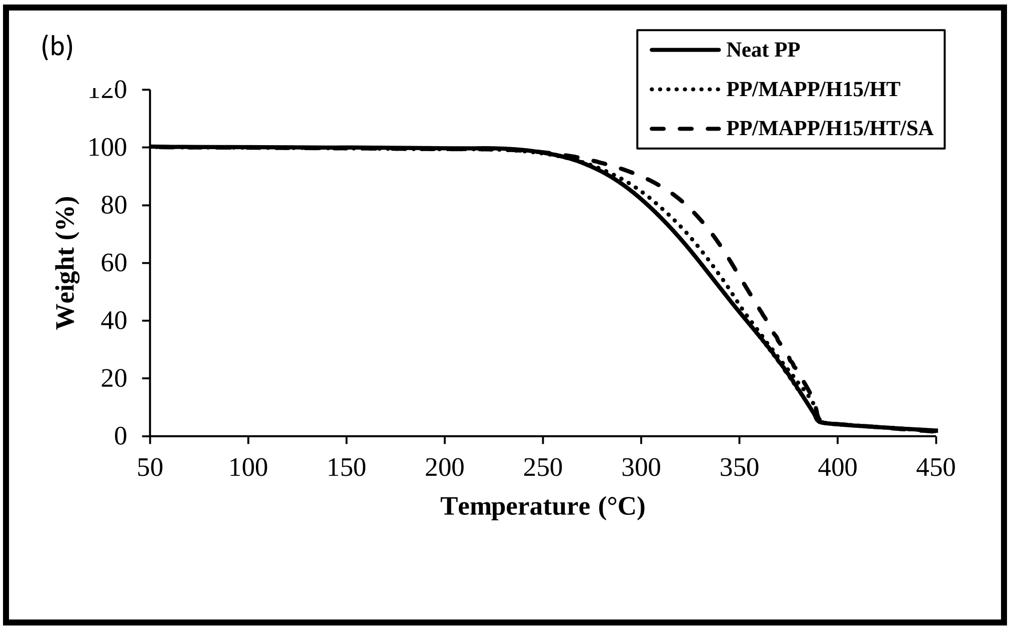

Fig. 12: TGA analysis of (a) fibre mats and (b) composites.

TGA curves for neat PP, composites with MAPP and with the combination of SA and MAPP are shown in Fig. 12b. The thermal degradation of neat PP and the composites was initiated at around 260 °C. The initial 10% of weight loss was at higher temperatures for composites (295 °C and 310 °C for the composites with MAPP only and combination of SA and MAPP treatment, respectively) than for neat PP (280 °C); the increased thermal stability of fibre improved that of PP. It has also been reported that the incorporation of fibres can immobilise free radicals formed as a result of the initiation of polymer degradation, improving the thermal stability of composites and hemp fibre inclusion has been seen to increase thermal resistance of PP elsewhere (Mofokeng et al. 2012).

3.7 Swelling studies

Interfacial strength between fibre and the matrix in composites can be correlated to swelling index. This is related to the presence of voids at weak interfaces, commonly promoting solvent uptake (Bhattacharya, Rawlins, and Ray 2008; Jacob, Thomas, and Varughese 2006). As can be seen in Fig. 13, the swelling indices for composites with SA only, composites with MAPP and the combination of SA and MAPP were lower compared to those composites with alkali only, supporting a further improvement for interfacial strength obtained. The composites coupled with MAPP had the lowest swelling index followed by composites with SA only. Swelling index for the composites with combination of SA and MAPP was slightly lower compared to the composites with MAPP only. However, this reduction was found to be insignificant (confirmed by Student's test).

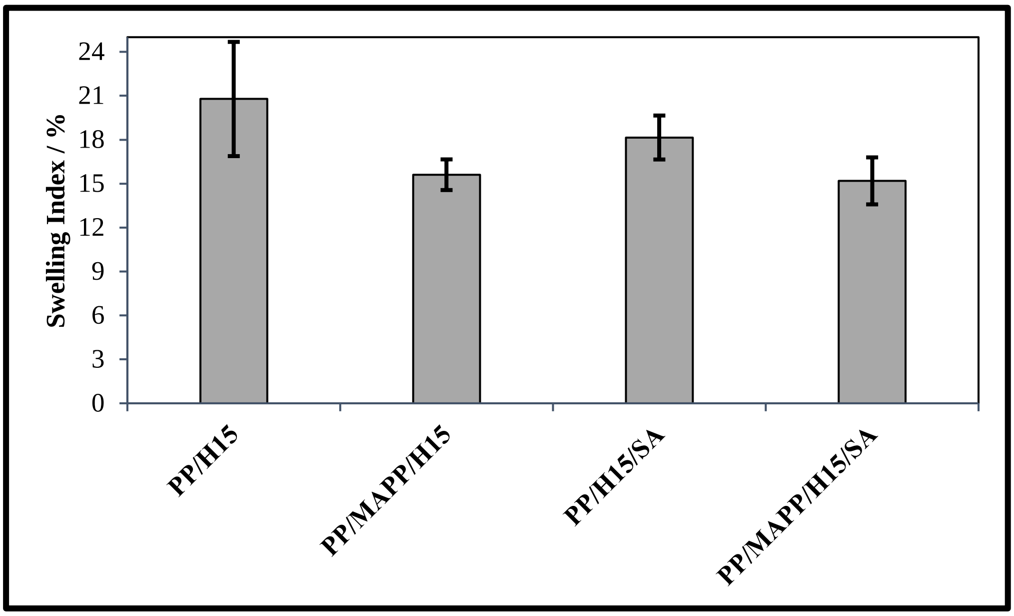

Fig. 13: Swelling index for hemp composites (fibre content of 15 wt%). Immersion of samples was 48 h.

4.0 Conclusions

Stearic acid vapour treatment brought about a weight percentage gain (0.54 %) with SEM providing evidence of modification at fibre surfaces in the form of a thin layer. SA treatment was found to increase thermal stability of fibres and drastically increase the contact angle with water indicating that the treatment strongly reduces their polar interaction ability.

Composites with MAPP coupling agent exhibited the highest tensile strength. However, in the absence of MAPP, the composites with fibres treated with stearic acid were significantly stronger (15 %) than the composites with fibres treated with alkali only. This indicates that stearic acid could act as a coupling agent through improving fibre wettability increasing the contact between fibre and matrix to improve strength, but not as effective as maleic anhydride polypropylene. Although the composites made with a combination of stearic acid and maleic anhydride polypropylene did not exhibit any additive benefits for tensile strength, there was a noticeable reduction in the standard deviation in tensile strength. This indicates potentially more reliable wetting of fibres by the matrix with the addition of stearic acid providing better uniformity of adhesion. Improved thermal stability was also seen for SA treated fibre composites. Stearic acid, being low cost and renewable, could be a viable alternative to maleic anhydride polypropylene in applications where maximising strength is not the only parameter being optimised, however caution would be needed in the presence of moisture. Additionally, stearic acid treatment using vapour is recommended, as it minimised the amount of stearic acid needed and avoids the need to use a solvent.

References

Azwa, ZN, BF Yousif, AC Manalo, and W Karunasena (2013) A review on the degradability of polymeric composites based on natural fibres. Mater. Des. 47:424-42.

Beckermann, Gareth (2007) Performance of hemp-fibre reinforced polypropylene composite materials.

Bhattacharya, Amit, James W Rawlins, and Paramita Ray (2008).Polym. Grafting Crosslinking John Wiley and Sons, Place.

Conceição, Isaías Damasceno da, Lucas Rafael Carneiro da Silva, Tatianny Soares Alves, Renata Barbosa, and Rômulo Ribeiro Magalhães de Sousa (2019) Investigation of the Wettability Using Contact Angle Measurements of Green Polyethylene Flat Films and Expanded Vermiculite Clay Treated by Plasma. Mater. Res. 22:

Dányádi, Lívia, János Móczó, and Béla Pukánszky (2010) Effect of various surface modifications of wood flour on the properties of PP/wood composites. Composites, Part A 41:199-206.

Dhakal, HN, ZY Zhang, and MOW Richardson (2007) Effect of water absorption on the mechanical properties of hemp fibre reinforced unsaturated polyester composites. Compos. Sci. Technol. 67:1674-83.

Efendy, MG Aruan, and KL Pickering (2014) Comparison of harakeke with hemp fibre as a potential reinforcement in composites. Composites, Part A 67:259-67.

Ghazali, Mohd, and Aruan Efendy. 2016. 'Bio-composites materials from engineered natural fibres for structural applications', University of Waikato.

Hernάndez, Yarazett, Tomas Lozano, Ana B Morales‐Cepeda, Fabiola Navarro‐Pardo, Maricela E Ángeles, Luisiana Morales‐Zamudio, José A Melo‐Banda, Sάul Sάnchez‐Valdes, Guillermo Martínez‐Colunga, and Francisco Rodríguez (2019) Stearic acid as interface modifier and lubricant agent of the system: Polypropylene/calcium carbonate nanoparticles. Polym. Eng. Sci. 59:E279-E85.

Huang, Lijie, Xiaoxiao Zhang, Mingzi Xu, Jie Chen, Yinghan Shi, Chongxing Huang, Shuangfei Wang, Shuxiang An, and Chunying Li (2018) Preparation and mechanical properties of modified nanocellulose/PLA composites from cassava residue. AIP Adv. 8:025116.

Jacob, Maya, Sabu Thomas, and KT Varughese (2006) Novel woven sisal fabric reinforced natural rubber composites: tensile and swelling characteristics. J. Compos. Mater. 40:1471-85.

Kabir, MM, H Wang, KT Lau, and F Cardona (2012) Chemical treatments on plant-based natural fibre reinforced polymer composites: An overview. Composites, Part B 43:2883-92.

Kalaprasad, G, Bejoy Francis, Selvin Thomas, C Radhesh Kumar, C Pavithran, Gabriël Groeninckx, and Sabu Thomas (2004) Effect of fibre length and chemical modifications on the tensile properties of intimately mixed short sisal/glass hybrid fibre reinforced low density polyethylene composites. Polym. Int. 53:1624-38.

Lamour, Guillaume, Ahmed Hamraoui, Andrii Buvailo, Yangjun Xing, Sean Keuleyan, Vivek Prakash, Ali Eftekhari-Bafrooei, and Eric Borguet (2010) Contact angle measurements using a simplified experimental setup. J. Chem. Educ. 87:1403-07.

Li, Xue, Lope G Tabil, and Satyanarayan Panigrahi (2007) Chemical treatments of natural fiber for use in natural fiber-reinforced composites: a review. J. Polym. Environ. 15:25-33.

Mofokeng, Julia Puseletso, AS Luyt, T Tábi, and J Kovács (2012) Comparison of injection moulded, natural fibre-reinforced composites with PP and PLA as matrices. J. Thermoplast. Compos. Mater. 25:927-48.

Pickering, Kim (2008).Properties and performance of natural-fibre composites Elsevier, Place.

Pickering, KL, MG Aruan Efendy, and TM Le (2015) A review of recent developments in natural fibre composites and their mechanical performance. Composites, Part A

Rachini, Ali, Marianne Le Troedec, Claire Peyratout, and Agnès Smith (2009) Comparison of the thermal degradation of natural, alkali ‐ treated and silane ‐ treated hemp fibers under air and an inert atmosphere. J. Appl. Polym. Sci. 112:226-34.

Raj, RG, BV Kokta, F Dembele, and B Sanschagrain (1989) Compounding of cellulose fibers with polypropylene: Effect of fiber treatment on dispersion in the polymer matirx. J. Appl. Polym. Sci. 38:1987-96.

Sunny, Tom, Kim L Pickering, and Shen Hin Lim (2020) Alkali treatment of hemp fibres for the production of aligned hemp fibre mats for composite reinforcement. Cellulose 27:2569-82.

Zafeiropoulos, NE, CA Baillie, and FL Matthews (2000) A study of the effect of surface treatments on the thermal stability of flax fibres. Adv. Compos. Lett. 9:096369350000900405.

Zafeiropoulos, NE, PE Vickers, CA Baillie, and JF Watts (2003) An experimental investigation of modified and unmodified flax fibres with XPS, ToF-SIMS and ATR-FTIR. J. Mater. Sci. 38:3903-14.

Zafeiropoulos, NE, DR Williams, CA Baillie, and FL Matthews (2002) Engineering and characterisation of the interface in flax fibre/polypropylene composite materials. Part I. Development and investigation of surface treatments. Composites, Part A 33:1083-93.

Zeng, Yuan-Xian, Xiu-Wen Zhong, Zhao-Qing Liu, Shuang Chen, and Nan Li (2013) Preparation and enhancement of thermal conductivity of heat transfer oil-based MoS 2 nanofluids. J. Nanomater. 2013:3.